

## Locally Modified Winds Regulate Circulation in a Semi-Enclosed Shelf Sea

 Anil Akpınar<sup>1,2</sup> , Matthew R. Palmer<sup>1</sup> , Mark Inall<sup>3</sup> , Barbara Berx<sup>4</sup> , and Jeff Polton<sup>1</sup> 
<sup>1</sup>National Oceanography Centre, Liverpool, UK, <sup>2</sup>Now at Institute of Marine Sciences, Middle East Technical University, Erdemli, Turkey, <sup>3</sup>Scottish Association of Marine Science, Oban, UK, <sup>4</sup>Marine Scotland Science, Aberdeen, UK

**Key Points:**

- Local modification of winds provides an important control on North Sea circulation
- Orography and ocean-atmosphere interaction are two important mechanisms contributing to the generation of wind stress curl extrema
- Local winds are shown to be more important than previously documented and may be more susceptible to change than prevailing winds

**Correspondence to:**

 A. Akpınar,  
akpinar.anil@gmail.com

**Citation:**

 Akpınar, A., Palmer, M. R., Inall, M., Berx, B., & Polton, J. (2022). Locally modified winds regulate circulation in a semi-enclosed shelf sea. *Journal of Geophysical Research: Oceans*, 127, e2021JC018248. <https://doi.org/10.1029/2021JC018248>

Received 16 NOV 2021

Accepted 9 MAR 2022

**Author Contributions:**
**Conceptualization:** Anil Akpınar, Matthew R. Palmer, Mark Inall, Barbara Berx, Jeff Polton

**Formal analysis:** Anil Akpınar

**Investigation:** Anil Akpınar, Matthew R. Palmer, Mark Inall, Barbara Berx, Jeff Polton

**Methodology:** Anil Akpınar, Matthew R. Palmer, Mark Inall, Barbara Berx, Jeff Polton

**Software:** Anil Akpınar

**Validation:** Matthew R. Palmer, Mark Inall, Barbara Berx, Jeff Polton

**Visualization:** Anil Akpınar

**Writing – original draft:** Anil Akpınar, Matthew R. Palmer

**Writing – review & editing:** Matthew R. Palmer, Mark Inall, Barbara Berx, Jeff Polton

© 2022. The Authors.

 This is an open access article under the terms of the [Creative Commons Attribution License](https://creativecommons.org/licenses/by/4.0/), which permits use, distribution and reproduction in any medium, provided the original work is properly cited.

**Abstract** Wind driven circulation in the North Sea is revisited with a specific focus on locally modified winds and their impacts. We show for the first time that local extrema of the wind stress curl (WSC), generated by orography and ocean-atmosphere interactions, help regulate circulation in the northern North Sea. While calculated transports are strongly coupled with wind stress, which itself is driven by large-scale forcing, transports through the Norwegian Trench have higher correlations with the WSC field due to local extrema. Such WSC extrema regulate the eddy activity around the Norwegian Trench. We conclude that orography and ocean-atmosphere interaction are two important mechanisms contributing to the generation of the WSC extrema around the Norwegian coast. Ocean-atmosphere interaction is considered a potential mechanism developing the WSC extrema. Our results show that local winds are more important than previously documented, with important implications for regional circulation likely to result from future changes to local surface gradients, such as may arise from changing meteorological or hydro-climatic forcing. These are additional impacts on North Sea circulation that may not be accounted for from changes in wind stress alone.

**Plain Language Summary** North Sea circulation is investigated with a specific focus on the local winds and their impacts. We show for the first time that the local extrema of the wind field, generated by the coastline and oceanic contributions, help regulate circulation in the northern North Sea. Wind is driven by large-scale forcing mechanisms, and is closely related with volume transports. Volume transports through the Norwegian Trench are better related to the wind field, due to local extrema of wind. Local extrema of wind, and their direction, stimulates rotation in the region, controlling the eddy activity around the Norwegian Trench. We conclude that interaction of winds with the land and an ocean-atmosphere feedback mechanism contribute to the generation of the local extrema of wind along the Norwegian coastline. Our results show that local winds are more important than previously known and have important implications for regional circulation. Therefore, future changes to local density differences from changing meteorological conditions may have further impacts on North Sea circulation, which may not be accountable from changes in wind stress alone.

### 1. Introduction

The North Sea is surrounded by approximately 184 million inhabitants that inevitably rely on its blue economy, placing it among the world's most human influenced marine ecosystems (Halpern et al., 2008; Moullec et al., 2021). Additionally, the North Sea is a hotspot for climate change having large seasonal shifts and trends in climate change indicators above the global average (Burrows et al., 2011; Degraer et al., 2019; Holt et al., 2012), and so provides an indicator of change for the wider North West European continental shelf.

The North West European continental shelf plays an important role as a sink for atmospheric carbon dioxide (Frankignoulle & Borges, 2001). The North Sea has been shown to be a particularly efficient component of this system, exporting most of the regional oceanic CO<sub>2</sub> extracted from the atmosphere during summer months off the continental shelf to the deeper waters of the Atlantic Ocean (Thomas et al., 2005) via down-welling circulation (Holt et al., 2009). North Sea circulation is therefore a critical component of the North West European shelf seas biological carbon pump. In return, Atlantic inflow has a conditioning influence on the physical structure (Marsh et al., 2017; Sheehan et al., 2017) and biogeochemistry of the North Sea (Mathis et al., 2019). On inter-annual timescales variations in temperature and salinity in the North Sea have been shown to correlate significantly with the AMO (Atlantic Multidecadal Oscillation), and flow strengths with the NAO (Johnson et al., 2020). Recent studies however, have indicated potential blocking of Atlantic connectivity (Holt et al., 2018) in future climate scenarios with subsequently dramatic implications for the health and productivity of the North Sea (Wakelin

et al., 2020). Wind stress is an important forcing mechanism to consider for North Sea exchange with the Atlantic, as it is identified as the major driver of regional circulation (Huthnance, 1991). Changes in the strength and direction of prevailing winds can induce a reversal in circulation (Stanev et al., 2019), and even blocking (Christensen et al., 2018). Additionally, wind has implications for the biogeochemistry: driving inter-annual to decadal variability in nutrient concentrations in the northern North Sea (Pätsch et al., 2020). Changing winds also have an impact on budgets of carbon (Kühn et al., 2010) and nutrient (Pätsch & Kühn, 2008). A thorough understanding of regional wind variability is therefore essential to understand North Sea circulation, regional biogeochemistry, and future impacts from changing hydro-climatic forcing.

Previous North Sea studies have shown the importance of large-scale winds (Winther & Johannessen, 2006), as well as the topographic modification of wind-driven circulation around the Norwegian Trench (Davies & Heaps, 1980) but local wind forcing and its impacts on regional circulation remain poorly documented. The Norwegian Trench is a frontal area maintained by freshwater influence from the Baltic outflow and numerous riverine inputs, with instabilities leading to meanders and eddy generation (Johannessen et al., 1989). This area is subsequently a prime candidate for ocean-atmosphere interaction since mesoscale ocean-atmosphere interactions are well documented in the vicinity of fronts both over the open-ocean (e.g., Chelton & Xie, 2010; O'Neill et al., 2010) and global coastal ocean (e.g., Wang & Castelao, 2016). Blowing parallel to a sea surface temperature (SST) front, wind accelerates (decelerates) over warm (cold) water, resulting in wind stress curl and divergence anomalies (O'Neill et al., 2010), which are related to crosswind and downwind components of the SST gradient (Chelton et al., 2007).

In this study, we investigate local extrema of wind stress curl observed around the Norwegian coast and consider their implications for local and regional (i.e., northern North Sea) circulation. First, we investigate the impact on both large-scale and mesoscale circulation. Second, we investigate causes of the local WSC extrema, considering orography and ocean-atmosphere interaction as potential drivers.

## 2. Materials and Methods

Data used in this study are provided by the approximately 7 km reanalysis product (Atlantic Margin Model, AMM7: North-West Shelf Monitoring and Forecasting Center; NWS-MFC, 2021) and the approximately 1.5 km forecast product (AMM15: Crocker et al., 2020; Lewis et al., 2019; NWS-MFC, 2020; Tonani et al., 2019) for the North-West European Shelf Seas, distributed freely by CMEMS (Copernicus Marine Environment Monitoring Service). Both products are configurations of the NEMO (Nucleus for European Modelling of the Ocean; Madec and the NEMO Team, 2016) model. Atmospheric forcing is ECMWF (European Centre for Medium-Range Weather Forecasts) ERA5 fields for AMM7 (NWS-MFC, 2021) and ECMWF Integrated Forecasting System (IFS)-Atmospheric Model High Resolution (HRES) operational Numerical Weather Prediction forecast fields for AMM15 (NWS-MFC, 2020). In Section 3.1, we use AMM7 to demonstrate the large-scale circulation and in Section 3.2 we use AMM15 to investigate the (sub)mesoscale circulation in the North Sea. Submesoscales are not fully resolved in this study, as we use monthly mean fields, hence the term “sub-mesoscale” used in this study refers to spatial scales (<10 km) only, and does not address short-lived submesoscale features.

In Section 3.1, monthly mean fields of the AMM7 model were used for 1993–2019. The AMM15 model was available as daily mean fields for 2017–2019. In Section 3.2, daily AMM15 fields were averaged into monthly means for coherence with the AMM7 analysis. Volume transports were calculated using the following formula:

$$VT_{\text{positive/negative}} = U_n * dx * h$$

$$VT_{\text{net}} = VT_{\text{positive}} + VT_{\text{negative}}$$

where VT stands for volume transport,  $U_n$  is the normal velocity component,  $dx$  is the grid spacing, and  $h$  is the layer thickness at position of normal velocity. Positive (negative) volume transport denotes transports in the same (opposite) direction as the arrows shown in Figure 1. Net transport is the sum of positive and negative transports. Volume transport was calculated from time mean velocity fields, and potentially misses contributions due to tidal variability. Given close agreement with previous estimates by O'Dea et al. (2017), we consider these to be minor. All “transports” presented in this study refer to the net volume transport, units of Sv ( $1 \text{ Sv} = 10^6 \text{ m}^3 \text{ s}^{-1}$ ). Transect positions were chosen from those already prescribed by the North West Shelf Operational Oceanographic System

**Table 1**  
*Coordinates Defining the NOOS Transects*

Transect number	Transect name	From		To	
		Latitude	Longitude	Latitude	Longitude
1	Shetland North	60°41'N	0°55'W	60°41'N	3°00'E
2	Sognesjoen	60°41'N	3°00'E	60°41'N	6°00'E
4	Orkney	59°17'N	2°30'W	59°17'N	3°20'E
5	Utsira	59°17'N	3°20'E	59°17'N	6°30'E
7	Aberdeen	57°08'N	2°15'W	57°08'N	5°00'E
8	Hanstholm West	57°08'N	5°00'E	57°08'N	8°40'E

(NOOS; O’Dea et al., 2017; NOOS Team, 2013) (Figure 1) and relate to Transect 1 (T1-Shetland North), Transect 2 (T2-Sognesjoen), Transect 4 (T4-Orkney), Transect 5 (T5-Utsira), Transect 7 (T7-Aberdeen), Transect 8 (T8-Hanstholm west). Net transport for Transect 1, Transect 4, and Transect 7 (Figure 1) is defined as positive into the North Sea, which is counter to the definition of NOOS for these transects (NOOS Team, 2013). Transition between the shallow and deep transects corresponds to the 200 m depth contour. Coordinates of the NOOS transects have been provided in Table 1.

Northern North Sea transports (Table 1, Transects 1–5) account for the majority of exchanges with the Atlantic Ocean (Winther & Johannessen, 2006). Transports through other transects north and south of T4 and T5 showed similar temporal variability and so only the results from these two transects are presented to represent the link between transports and wind forcing in the northern North Sea.

Monthly mean SST and wind (10 m eastward and northward components) data were obtained from ERA5 reanalysis (Copernicus Climate Change Service [C3S], 2017). Zonal and meridional wind stress were computed in addition to the wind stress curl (hereon WSC).

The WSC field was inherently noisy, so was decomposed into its major components using EOF (Empirical Orthogonal Function) analysis. The first principal component (PC-1) was most significant, explaining 48% of the total variability, and was therefore used for calculating the WSC correlations with transport. Statistical significance of correlations presented in this study is calculated following a random phase test (Ebisuzaki, 1997). All presented correlation coefficients are statistically significant at the 95% confidence level, unless specified otherwise.

Following previous studies (Chelton et al., 2007; Desbiolles et al., 2014; Wang & Castelao, 2016) cross-wind SST gradients were calculated by decomposing the SST gradient vector:

$$\nabla \text{SST} \times \hat{k} = \nabla \text{SST} * \sin \theta$$

where  $\hat{k}$  is the unit vector in the direction of the wind stress and  $\theta$  is the counter clockwise angle from the SST gradient vector to  $\hat{k}$ . Monthly North Atlantic Oscillation (NAO) Index was obtained from Hurrell et al. (2020).

### 3. Results

#### 3.1. Wind Regulated Volume Transport

The 27-year monthly net volume transport across the selected NOOS transects (Figure 2) present a clear seasonal cycle with maxima in winter. The period mean (1993–2019) transport was 0.82 Sv (1 Sv = 10<sup>6</sup> m<sup>3</sup> s<sup>-1</sup>) across T4 and 1.00 Sv across T5. The volume transport across northern transects are well correlated with the first principal component of the zonal wind stress, with a correlation coefficient  $r = 0.84$  (zero lag) and  $r = 0.85$  (zero lag) for T4 and T5, respectively. These results demonstrate that seasonal circulation in the northern North Sea, including the inflow of Atlantic water is closely correlated with westerly winds. The WSC likely provides a better representation of local wind forcing as it represents both the zonal and meridional wind stress. Meridional wind stress becomes enhanced around the Norwegian coast. The WSC (first principal component) consequently displays a dipole extremum around the Norwegian coast, with a positive (cyclonic) maximum around southern Norway and negative (anti-cyclonic) maximum around the northwest (north of approximately 61°N) Norwegian coast, with approximately 60°N being an apparent focal point (Figure 1a).

Figure 2a shows the transport through T4 and T5 alongside the first principal component (PC-1) of WSC. Correlation between the WSC PC-1 and transport is  $r = 0.78$  (zero lag) for T4 and  $r = 0.88$  (zero lag) for T5.

Transport is enhanced during winter periods when the regional wind field is intensified. The maximum transport for both transects was observed in winter 1993, which corresponds to the maximum observed value of positive WSC EOF value. However, it is not possible to explain every peak in the transport time-series solely from wind. For example, minimum transport values for T4 in November 2000 do not correspond to a WSC minimum.

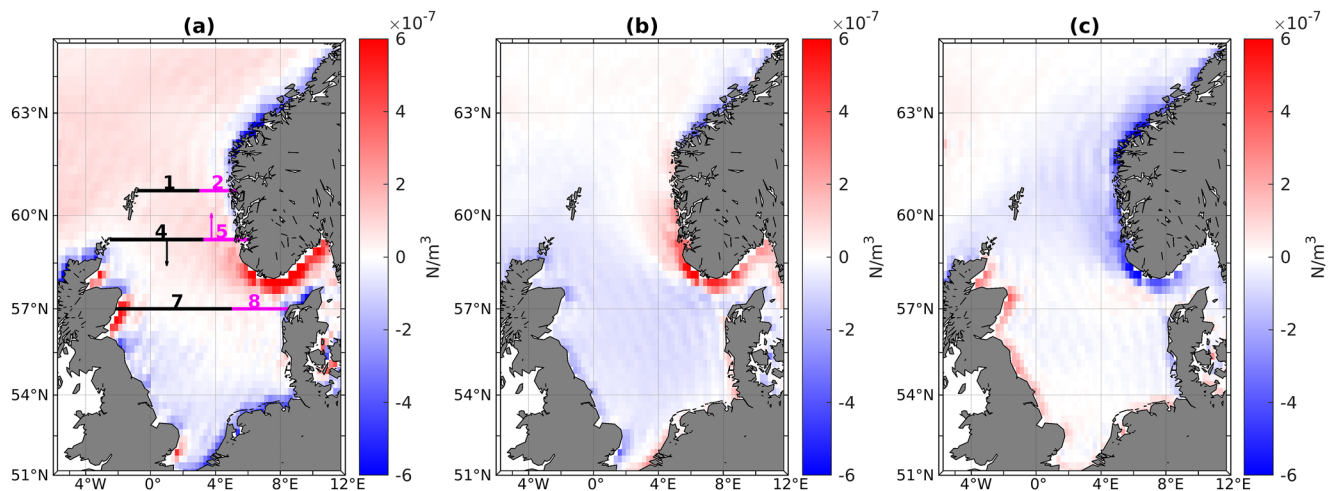


**Figure 1.** (a) First EOF mode of WSC (variance explained: 48%) with NOOS transects overlaid. (b) Second EOF mode of WSC (variance explained: 21%) (c) Third EOF mode of WSC (variance explained: 16%). Principal components associated with the EOF modes are shown in Figure 2 (PC-1) and Figure 5 (PC-2 and PC-3). Positive WSC is defined as anti-clockwise.

Interestingly, this date corresponds to a reversal in the direction of net transport (negative values). Nevertheless, these time series and their high correlations demonstrate how the wind generally provides a primary control on regulating regional seasonal circulation. Positive WSC EOF values correspond to enhanced positive transport, which represents flow into the North Sea (through T4) and outflows to the northern Atlantic through T5, which describes much of the seasonal cyclonic circulation in the northern North Sea.

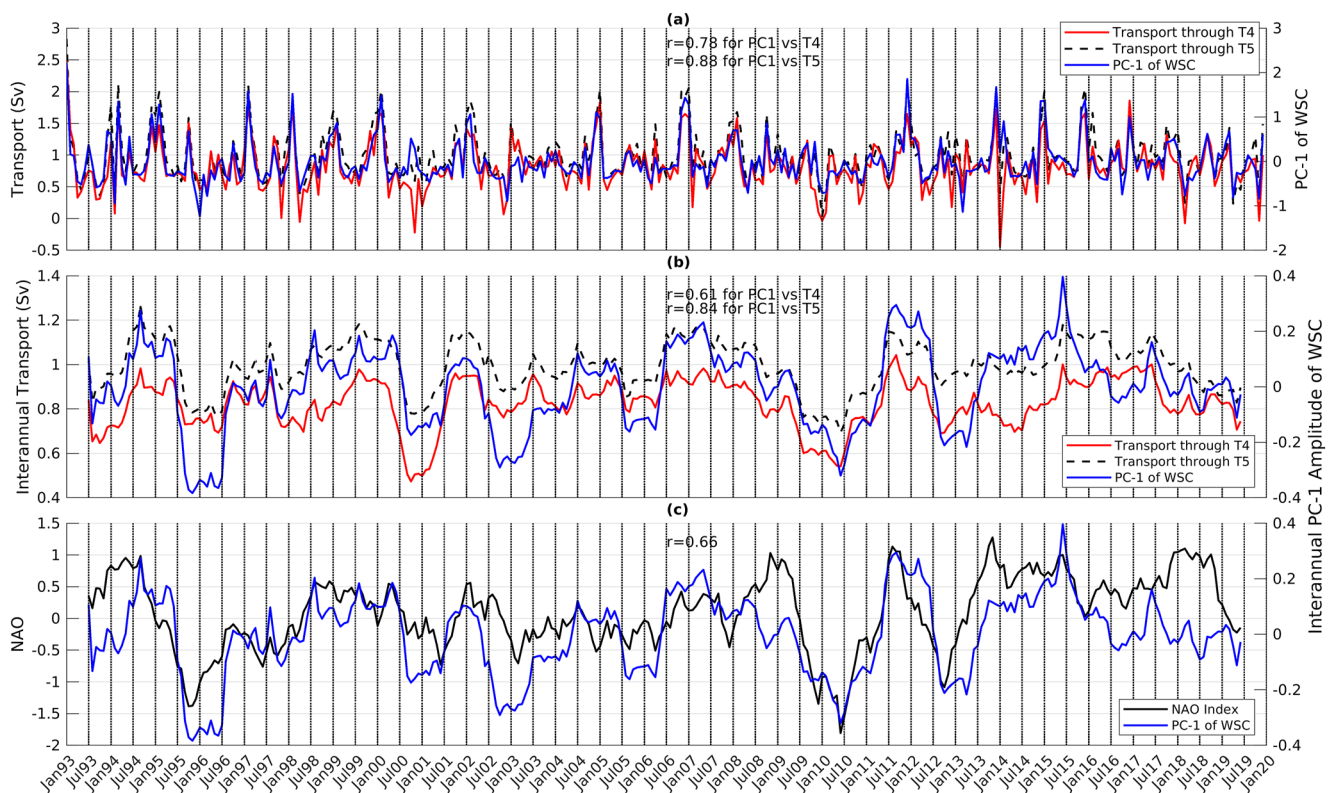


**Figure 2.** (a) Volume transport through T4 (black dashed line) and T5 (red line), as well as the first principal component (PC-1) of WSC (blue line). (b) Interannual volume transport through T4 (black dashed line) and T5 (red line) as well as PC-1 of WSC (blue line). (c) NAO (black line) and PC-1 of WSC (blue line). For (b) and (c), all time-series are low-pass filtered with a 1 year moving window.

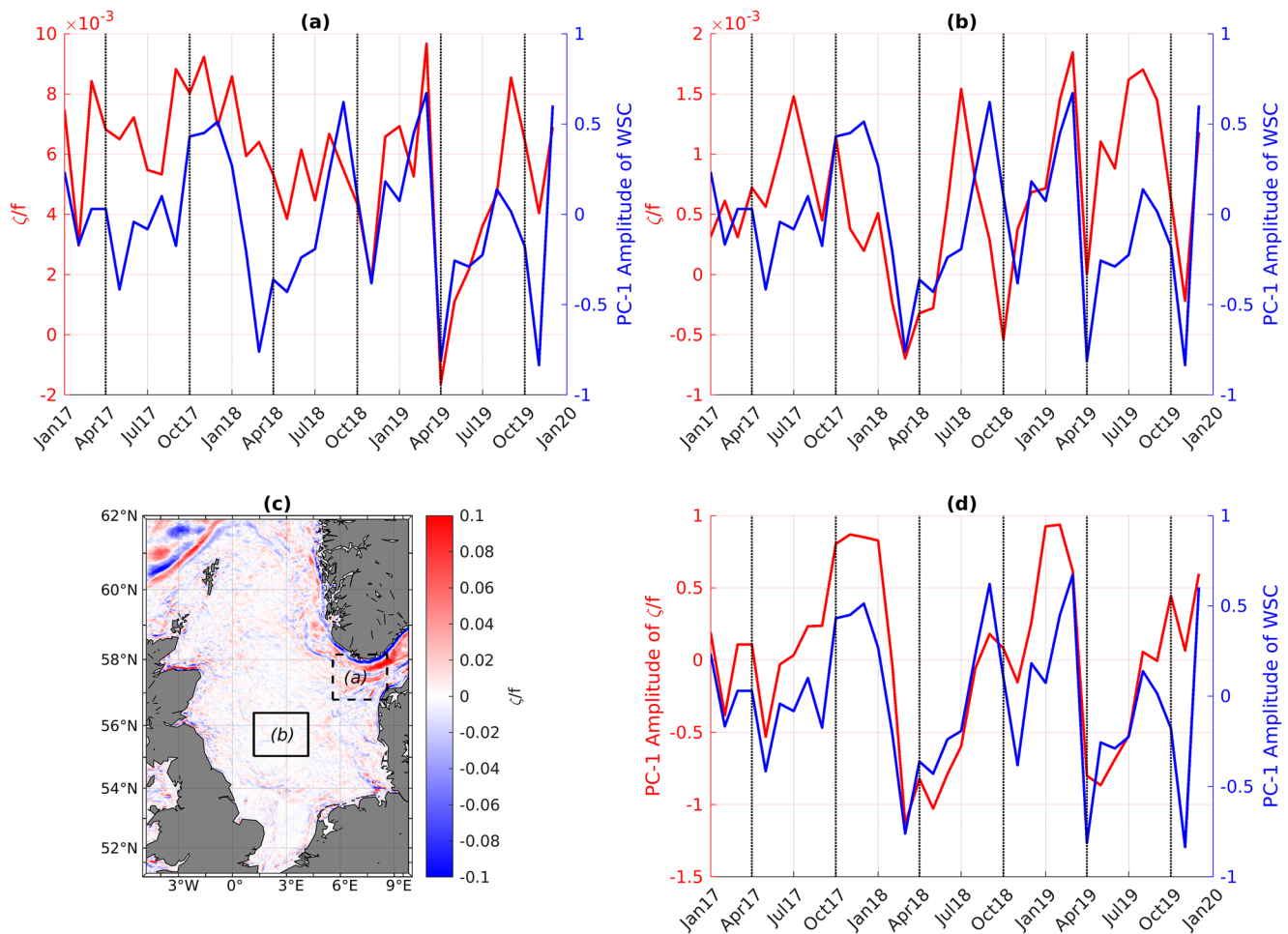


**Figure 3.** (a) Normalized relative vorticity in Norwegian Trench (area mean of dashed square in c) and PC-1 of WSC. (b) Normalized relative vorticity in Central North Sea (area mean of solid square in c) and PC-1 of WSC. (c) First EOF mode of normalized relative vorticity. Dashed square and solid square are the areas used to calculate the mean normalized relative vorticity for the Norwegian Trench (a) and Central North Sea (b), respectively. (d) PC-1 of normalized relative vorticity and PC-1 of WSC.

To identify interannual variability, the seasonal signal was removed using a low-pass filter (1-year moving average) for both transports and WSC. The strongest correlation in all NOOS transects (Transects 1 to 8) between transport and WSC was observed at T5 in the Norwegian Trench, denoting the significance of the local WSC extrema interannually. Figure 2c clearly shows the negative NAO periods in 1996 and 2010 and 2012, causing negative WSC amplitude and reduced transport, whereas 2007 and 2011 showed an opposite signal. Transports were well correlated ( $r = 0.61$  for T4 and  $r = 0.82$  for T5, both maximal with 1-month lag) with the interannual component of WSC proving a close match with the wind regulated circulation. The WSC was well correlated with the NAO ( $r = 0.66$ , zero lag), in line with its role as the large-scale driver of regional and local wind fields. Variability at seasonal and interannual timescales are presented here, but higher frequency variability was not investigated.

### 3.2. Wind Driven Eddy Activity

Data from the eddy resolving model (AMM15) show WSC extrema around the Norwegian Trench impacts eddy activity in the region, with strong coupling between the WSC strength and relative vorticity (Figure 3). Positive WSC amplitudes correspond well with positive relative vorticity temporally. Correlations between WSC PC-1 and relative vorticity are presented for two areas (squares in Figure 3c): the Norwegian Trench (Figure 3a) and central North Sea (Figure 3b). In both cases, the calculated relative vorticity demonstrates some agreement with WSC;  $r = 0.43$  (zero lag) for Central North Sea (Figure 3c, solid square) and  $r = 0.58$  (zero lag) for Norwegian

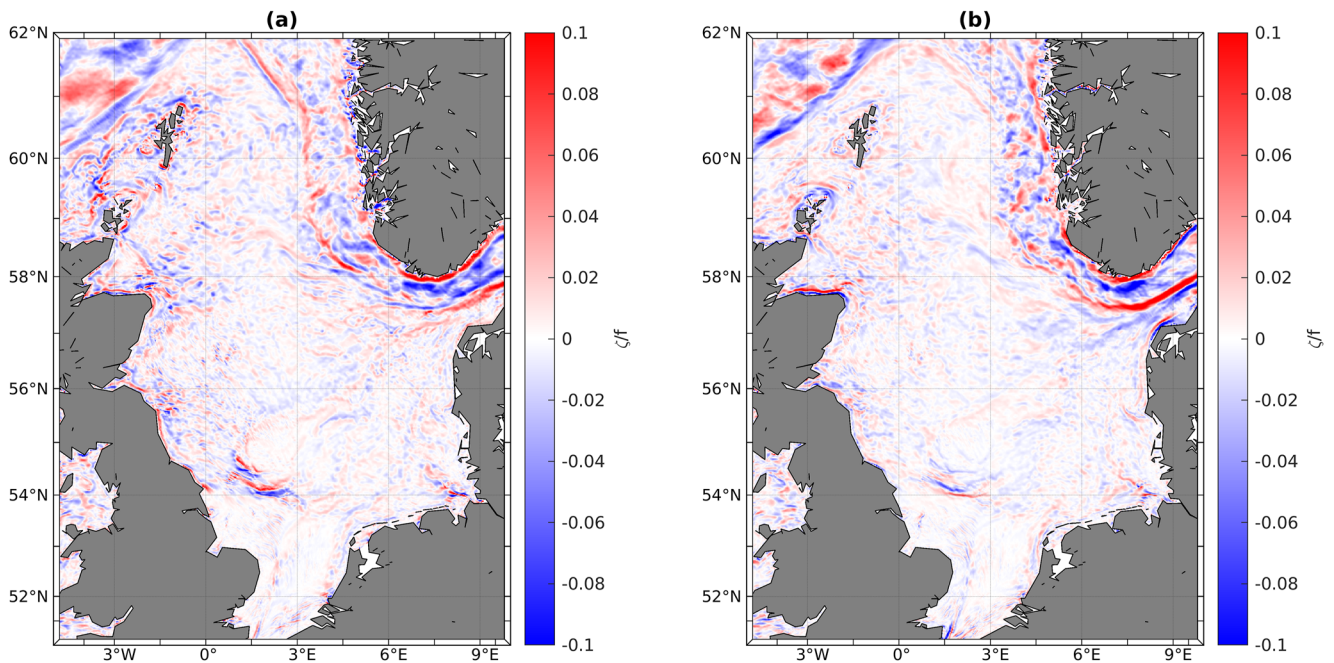


**Figure 4.** (a) Second EOF mode of normalized relative vorticity (b) Third EOF mode of normalized relative vorticity.

Trench (Figure 3c, dashed square), which undergoes significant variability over time (not shown, but highest in 2018). Area-mean representation of relative vorticity is prone to signal erosion as positive and negative features negate each other in the spatial mean. For a better representation of the eddy activity, here we use the EOF decomposition of relative vorticity normalized by Coriolis, which is a common proxy for eddy activity. Figure 3c represents the spatial distribution of the first principal component, which represents 27% of the total variability and shows strong (sub)mesoscale activity around the Norwegian coastline. Temporally (Figure 3d), it is well correlated with WSC PC-1 ( $r = 0.76$ , zero lag). Figure 4 represents the spatial distribution of the second (Figure 4a) and third (Figure 4b) principal components, which represent 19% and 15% of the total variability respectively. Temporally, the second mode of relative vorticity has statistically insignificant correlation ( $r = 0.49$  with 3-month lag) with WSC PC-1. The third mode of relative vorticity also has good correlation ( $r = 0.45$ , zero lag) with WSC PC-1. By its nature, spatial patterns of relative vorticity are highly turbulent but regardless of the spatial pattern of relative vorticity, it is well correlated with WSC PC-1, as shown by the correlation coefficients.

### 3.3. Regional Wind Stress Curl Variability and Its Drivers

Regionally, the majority of WSC variability is shown to arise from the zonal wind stress, with their first principal components (PC-1) being tightly coupled ( $r = 0.93$ ), whereas meridional wind stress has a weaker coupling ( $r = 0.43$ ) with WSC. An additional EOF analysis confined to the Norwegian Trench area (with the rest of the North Sea being masked) shows that locally around the Norwegian coastal area, correlation between zonal wind stress PC-1 and WSC PC-1 is considerably reduced ( $r = 0.57$ ) and correlation between meridional wind stress PC-1 and WSC PC-1 increases ( $r = 0.85$ ).

In total, the first three EOF modes represent approximately 85% of the total WSC variability. All three modes show a local WSC pattern around Norway. The first EOF mode of WSC explains 48% of the total variability and shows well organized dipole extremum around the Norway coast (Figure 1). The magnitude of both the spatial mode (Figure 1a) and PC (Figure 2a) of the first EOF mode are larger than those of second and third EOF modes (Figure 5). The temporal variability of PC-1 (Figure 2), however, displays interannual oscillation between positive and negative values that are well correlated to the NAO. Positive values of PC result in enhanced extrema of the dipole WSC pattern, whereas negative values of PC create a weaker dipole pattern. The first EOF mode (Figure 1a) is mostly positive in the northern North Sea (with the exception of coastal features) which leads to enhanced (reduced) cyclonic circulation when its PC is positive (negative).

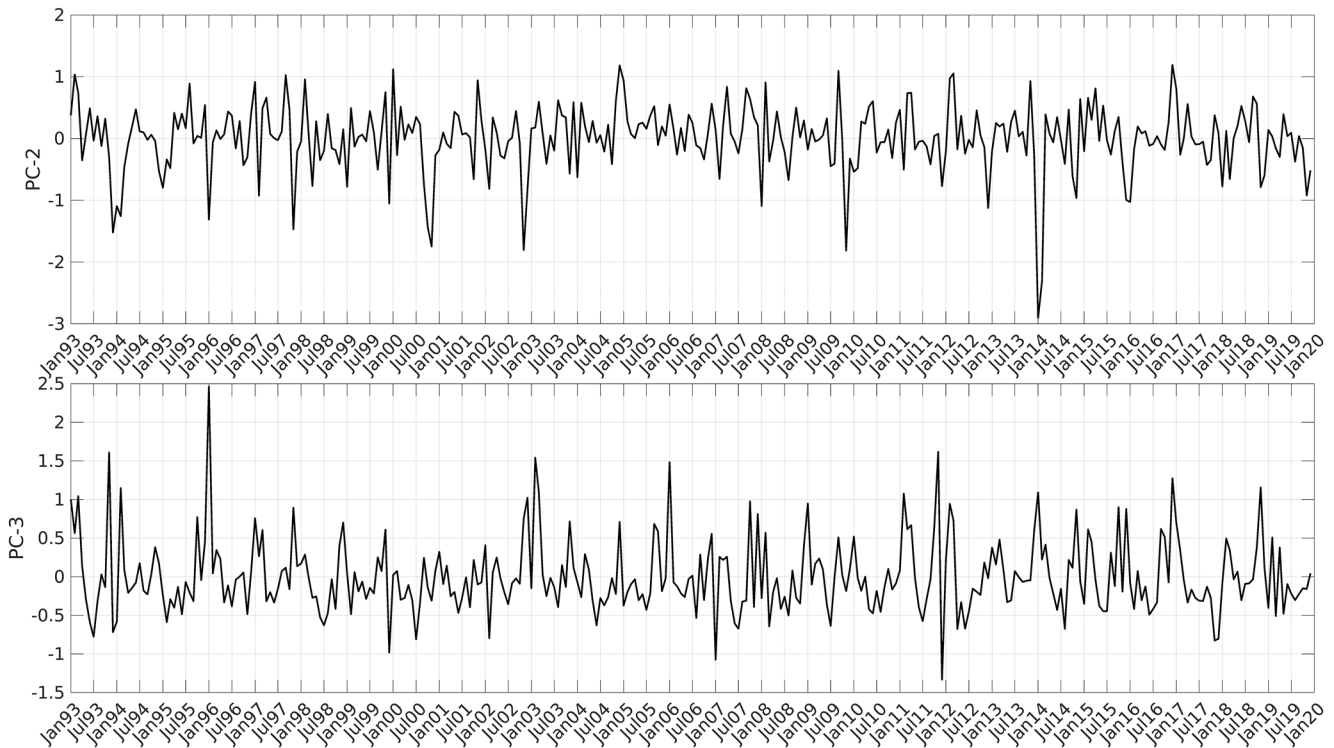


**Figure 5.** (a) Second principal component (PC-2) of WSC. (b) Third principal component (PC-3) of WSC.

Second and third EOF modes of the WSC explain 21% and 16% of the total variability, respectively. Similar to the first mode, the second EOF mode displays a dipole pattern around Norway, with a change of sign at approximately 62°N, around 2° latitude difference from that of the first mode. The second mode (Figure 1b) displays a generally negative pattern for the majority of the North Sea with positive values most evident in Norwegian coastal waters (south of approximately 62°N) and extending through much of the Norwegian Trench. The second principal component (Figure 5a) displays positive (negative) values which correspond to enhanced cyclonic (anti-cyclonic) WSC around the Norwegian Trench. The western boundary of the positive WSC field in the second mode (Figure 1b) corresponds to the western boundary of the Norwegian Trench, however, no direct relationship was identified with transports across the NOOS transects.

The third EOF mode (Figure 1c) demonstrated a different distribution to the first two modes but was not found to have any direct relationship with the transports across the NOOS transects. The third principal component (Figure 5b) has both negative and positive values, with the positive (negative) values resulting in an enhanced anticyclonic (cyclonic) WSC around Norway.

In order to assess the possible physical mechanisms leading to the observed EOF spatial patterns, we have correlated each wind directional component time-series (324 months in total) with the observed EOF modes. The first EOF mode of WSC was found to be closely coupled with southwesterly winds ( $r = 0.92$  with a degree of freedom = 140, zero lag). The second EOF mode was closely linked with southeasterly winds ( $r = 0.72$  with a degree of freedom = 72), whereas the third EOF mode was found to show the highest correlation ( $r = 0.4$  with a degree of freedom = 88) with northerly winds (northeasterly and northwesterly combined).

These results clearly demonstrate the local modification of the WSC around Norway. Potential mechanisms for this WSC pattern are small-scale regional winds, orographic steering, and ocean-atmosphere interaction. The resolution of our data (0.25°) restricts this study to consider only the last two mechanisms; orography and ocean-atmosphere interaction.

Statistically significant correlations between SST and WSC (Figure 6b), and between crosswind SST gradients (CWSST) and WSC (Figure 6a) suggest a potential feedback mechanism between these variables. SST-WSC correlations (Figure 6b) reach a maximum around the Norwegian coast ( $r > 0.35$ ). Correlations (Figure 6a)

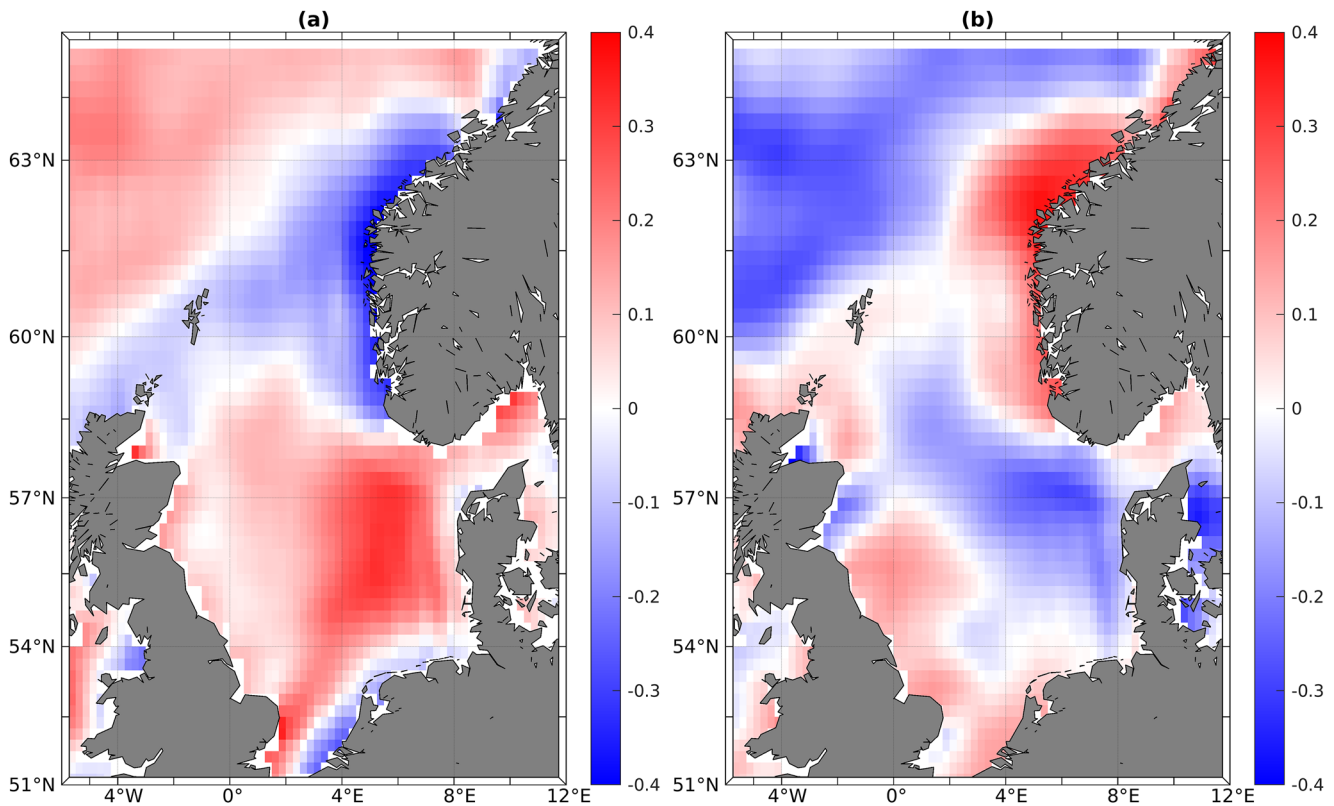


**Figure 6.** (a) Map of pointwise correlation coefficients ( $r$ ) between CWSST gradients and WSC. (b) Map of pointwise correlation coefficients ( $r$ ) between SST and WSC. For both (a) and (b), correlation coefficients are calculated for each pixel individually. All variables have been spatially filtered (using a two grid point square window) prior to the calculation of correlation coefficients.

between CWSST and WSC were slightly higher ( $r > 0.4$ ). Positive (negative) correlations suggest that increased surface temperature gradients correspond to enhanced positive (negative) WSC anomalies. Regardless of the sign convention, these correlations document ocean-atmosphere interaction in the region, with the potential for influencing regional scale circulation.

Seasonally, the highest CWSST-WSC correlations were found in winter, corresponding to intense temperature gradients that formed around the Norwegian Trench. Coupling coefficients were calculated as the slope of linear regressions between CWSST and WSC (following Chelton et al., 2007). Further assessment of seasonality was achieved via sequential filtering of coupling coefficients (following Legaard & Thomas, 2007; Wang & Castelao, 2016). Monthly time series were first low-pass filtered using a 12-month window. Subtracting the low-pass time-series from the original data set results in a time-series corresponding mostly to seasonal and higher frequencies. A second filter was applied (6-month low-pass filter) to obtain the seasonal time series (Wang & Castelao, 2016). Removing interannual and seasonal time series from the original time series leaves a residual time-series consisting of higher frequencies (intra-seasonal). Intra-seasonal (<6 months) variability was the dominant signal in the coupling coefficients time series.

## 4. Discussion

### 4.1. Wind Regulated Volume Transport

Transport was calculated using time-mean currents, therefore missing a component, separating our results from those of an absolute transport calculation. However, transport estimates presented here have the same order of magnitude as previous studies (O'Dea et al., 2017) and zonal wind stress was confirmed as the dominant forcing mechanism of transport and subsequently circulation in the northern North Sea, a re-affirmation of previously known studies (Huthnance, 1991; Otto et al., 1990). WSC was used as a proxy for the combined zonal and

meridional wind stress, the latter being shown to be locally important around the Norwegian trench and coast. Correlations between transports and WSC were found to be higher than those with simply zonal wind in the north-eastern part of the North Sea, implying the local importance of meridional wind stress as a driving mechanism for transport in the northeast and subsequently in regional circulation. Our approach, using space-time decompositions of wind forcing instead of mean fields, is not limited to large-scale wind but also includes local wind fields that are shown here to be important, as proposed in previous studies (Winther & Johannessen, 2006). The principal component of WSC (PC-1) was well correlated with both transport and the vorticity around Norwegian coastline. Westerly and northerly (easterly and southerly) winds enhance cyclonic (anticyclonic) circulation (Furnes, 1980). Correlation coefficients between transports and WSC were highest over seasonal periods (Section 3.1), but correlation was also high (minimum  $r = 0.61$ , at T4 with 1 month lag) interannually. Interannual variability of wind forcing was in good agreement ( $r = 0.66$ ) with the NAO, which provides a good indicator for the westerly winds (Iversen & Burningham, 2015). Shifts in the NAO index corresponds to changes in the wind regime, such as the one observed in 1996, where negative NAO resulted in reduced transport (Figure 2c) with further reported implications for the overall nitrogen and carbon budgets of the North Sea (Kühn et al., 2010; Pätsch & Kühn, 2008).

#### 4.2. Eddy Activity

AMM7 transport estimates indicate cyclonic circulation of the North Sea corresponds well with enhanced positive WSC (Section 3.1). The AMM7 configuration is not, however, sufficient to resolve mesoscale activity unlike AMM15, which was able to resolve some small-scale processes (Graham et al., 2018). AMM15 outputs reveal rich submesoscale activity, particularly in the Norwegian Trench, corresponding to both highest mean and eddy kinetic energy (supporting Røed & Fossum, 2004). Submesoscale activity is present at higher frequencies, and some eddies live shorter than 1 month but for this study, we only considered monthly means for compatibility with AMM7 temporal resolution. A general indicator of rotatory motion (relative vorticity normalized by Coriolis) showed good correlation with WSC in the central North Sea ( $r = 0.43$ , zero lag) and in the Norwegian Trench ( $r = 0.58$ , zero lag). Similarly, PC-1 of relative vorticity was in good correlation with WSC ( $r = 0.76$ , zero lag). PC-2 of relative vorticity (Figure 4a) has very low cross-correlations with WSC (reaching maximum  $r = 0.49$  with 3 months lag, statistically insignificant), whereas PC-3 of relative vorticity (Figure 4b) was in good correlation with WSC ( $r = 0.45$ , zero lag). These results suggest that eddy activity is coupled with WSC. However, it should be noted that our results do not fully resolve submesoscale activity, due to our monthly temporal resolution. Therefore, our results do not represent features at higher frequencies, yet they have previously been shown to be important for circulation in the region (Jacob & Stanev, 2017).

The generation of an anticyclonic eddy around Skaggerak was recently documented (Christensen et al., 2018), which is spatially coherent with the WSC anomaly presented here. Previously, eddy activity at the southern tip of Norway was linked with offshore veering of the Norwegian coastal current due to barotropic instability (Røed & Fossum, 2004). Considering the aforementioned good correlation between WSC and relative vorticity (Section 3.2), we suggest that the WSC provides a regulating control on eddy activity in the region surrounding the Norwegian Trench. Topography also plays a crucial role through conservation of potential vorticity, leading to re-distribution of the eddy field, although the exact role of topographic steering has been beyond the scope of this study and would require assessment through a series of controlled simulations.

#### 4.3. Origins of Wind Stress Curl Extrema

Potential mechanisms for the regional WSC extrema are: orography, small-scale regional winds, and ocean-atmosphere interactions. Synthetic Aperture Radar (SAR) data have revealed channeling winds through Norwegian fjords (Karagali et al., 2013), resulting in coastal wind variability around the Norwegian coast. We investigated the mesoscale winds ( $0.25^\circ$  data resolution), hence such small-scale winds are beyond our discussion and their exact contribution to regional WSC extrema remain an outstanding question, but mesoscale orographic modification of winds around the Norwegian coastline does remain a potential mechanism for the observed WSC extrema and warrants further investigation. Modeling studies (Barstad & Grønås, 2005) have confirmed regional modification of winds due to complex orography.

Ocean-atmosphere interaction, is the third possible reason for the observed regional extrema of WSC. If WSC drives upwelling, it is expected to be correlated with SST (as in Figure 6b), whereas if WSC is a result of ocean-atmosphere interactions, it is expected to be correlated with crosswind SST gradients (Castelao, 2012). Ocean-atmosphere (i.e., SST—Wind) interaction has previously been investigated for the global coastal ocean (Wang & Castelao, 2016). North-western European shelf ocean-atmosphere coupling has only been investigated for summer and was found to have intra-seasonal variability (Wang & Castelao, 2016). Our results are similar; intra-seasonal variability is the dominant signal in the time-series. However, seasonally, we have found highest ocean-atmosphere coupling in winter, corresponding to enhanced frontal gradients around Norwegian Trench. Winter also happens to be the season that shows highest instability in southern Norway, corresponding to outbreaks of low-salinity waters (Fossum, 2006).

Results here (Figure 6) show that WSC is, at times, well correlated with both SST and crosswind SST gradients, with the latter showing the strongest correlations and so indicating a predominance of ocean-atmosphere interaction in the region. In other words, the predominant regional mechanism for driving WSC is CWSST gradients (Figure 6b), with wind driven upwelling (Figure 6a) of secondary importance.

While the correlation is moderately high ( $r > 0.4$ ), coupling coefficients between WSC and CWSST gradients are erratic, with the dominant mode of variability being intra-seasonal, emphasizing the importance of higher frequencies in air-sea interaction as shown previously (Jacob & Stanev, 2017). Previous studies have used ERA products (Yu et al., 2020) and satellite products (Chelton et al., 2007; Wang & Castelao, 2016, among others) to quantify the ocean-atmosphere interaction. Yet, modeling (Boé et al., 2011; Jin et al., 2009) is required to quantify how much of the WSC variability is due to CWSST gradients (Castelao, 2012). Wind variability arising from orographic effects can be more important than that of wind variations associated with SST anomalies (Boé et al., 2011). This seems to be the case here, with the highest correlations (Figure 6) corresponding to regions of complex topography (mountains and fjords) around the western Norwegian coast (north of 62°N).

## 5. Conclusions

Local WSC extrema exist around the Norwegian coast, which are evident in the total WSC variability (represented by EOF modes). These local extrema are an important component of the WSC field in the North Sea. Our results suggest transports are highly coupled with wind forcing on monthly timescales. Correlation coefficients between transports and WSC are higher around the Norwegian Trench, indicating the importance of local wind forcing. We conclude therefore that local wind forcing is critical for a complete understanding North Sea circulation. Using WSC (notably its EOF decompositions) as a representation of the wind forcing is advantageous over wind stress (i.e., NAO driven westerly wind stress), as it also represents local wind forcing. WSC is particularly important around the Norwegian Trench where it is a consequence of ocean-atmosphere coupling, and a local cause of upwelling (Section 3.3 and 4.3) and rotatory motion (Sections 3.2 and 4.2).

Simulations with high spatial resolution show ubiquitous submesoscale activity around the Norwegian Trench. Relative vorticity is correlated with WSC in the central North Sea, but higher correlations are present around the Norwegian Trench. Our results suggest that regional WSC extrema might therefore be the forcing mechanism for the regional eddy activity investigated by previous studies (Christensen et al., 2018; Røed & Fossum, 2004). WSC is well correlated with rotatory motion and therefore has potential implications for the carbon budget through vertical motions related to Ekman dynamics (Holt et al., 2009) and likely ageostrophic secondary circulations arising from frontogenesis (Røed & Fossum, 2004).

We conclude that orography and ocean-atmosphere interaction are two important mechanisms contributing to the generation of the WSC extrema around the Norwegian coast. While the exact contribution from either requires further investigation, this local wind forcing plays an important role in North Sea circulation and should be accounted for in future studies, particularly when considering exchanges with the Baltic Sea (Christensen et al., 2018; Haid et al., 2020; Stanev et al., 2018) and the Atlantic Ocean (Holt et al., 2018). This highlights that exchange estimates should only be derived from eddy resolving models where processes and dynamics are adequately resolved. This is particularly important for future projections, where changing wind fields are predicted (Pryor et al., 2006) that may have significant impacts on local WSC effects and therefore on regional circulation and exchange.

## Data Availability Statement

The model data used in this paper are available at E.U. Copernicus Marine Service Information (<https://resources.marine.copernicus.eu/products>), via the following links for AMM7 ([https://resources.marine.copernicus.eu/?option=com\\_csw&view=details&product\\_id=NWSHELF\\_MULTIYEAR\\_PHY\\_004\\_009](https://resources.marine.copernicus.eu/?option=com_csw&view=details&product_id=NWSHELF_MULTIYEAR_PHY_004_009)) and AMM15 ([https://resources.marine.copernicus.eu/?option=com\\_csw&view=details&product\\_id=NORTHWESTSHELF\\_ANALYSIS\\_FORECAST\\_PHY\\_004\\_013](https://resources.marine.copernicus.eu/?option=com_csw&view=details&product_id=NORTHWESTSHELF_ANALYSIS_FORECAST_PHY_004_013)). Hurrell North Atlantic Oscillation Index is available via (<https://climatedataguide.ucar.edu/climate-data/hurrell-north-atlantic-oscillation-nao-index-station-based>). ERA5 data were downloaded from Copernicus Climate Change Service ((C3S), 2017) and is available via (<https://doi.org/10.24381/cds.f17050d7>).

## Acknowledgments

The authors kindly thank the reviewers for their constructive comments and criticism. This study was funded by the NERC Alternative Framework to Assess Marine Ecosystem Functioning in Shelf Seas (AlterEco) project under Grant No. NE/P013902/1. The authors thank Dr. Yuntao Wang for sharing his expertise and fruitful discussion on ocean-atmosphere interactions. This study has been conducted using E.U. Copernicus Marine Service Information.

## References

- Barstad, I., & Grønås, S. (2005). South-westerly flows over southern Norway—mesoscale sensitivity to large-scale wind direction and speed. *Tellus A: Dynamic Meteorology and Oceanography*, 57(2), 136–152. <https://doi.org/10.1111/j.1600-0870.2005.00112.x>
- Boé, J., Hall, A., Colas, F., McWilliams, J. C., Qu, X., Kurian, J., & Kapnick, S. B. (2011). What shapes mesoscale wind anomalies in coastal upwelling zones? *Climate Dynamics*, 36(11–12), 2037–2049
- Burrows, M. T., Schoeman, D. S., Buckley, L. B., Moore, P., Poloczanska, E. S., Brander, K. M., et al. (2011). The pace of shifting climate in marine and terrestrial ecosystems. *Science*, 334(6056), 652–655. <https://doi.org/10.1126/science.1210288>
- Castelao, R. M. (2012). Sea surface temperature and wind stress curl variability near a Cape. *Journal of Physical Oceanography*, 42(11), 2073–2087. <https://doi.org/10.1175/jpo-d-11-0224.1>
- Chelton, D. B., Schlax, M. G., & Samelson, R. M. (2007). Summertime coupling between sea surface temperature and wind stress in the California current system. *Journal of Physical Oceanography*, 37(3), 495–517. <https://doi.org/10.1175/jpo3025.1>
- Chelton, D. B., & Xie, S. P. (2010). Coupled ocean-atmosphere interaction at oceanic mesoscales. *Oceanography*, 23(4), 52–69. <https://doi.org/10.5670/oceanog.2010.05>
- Christensen, K. H., Sperrevik, A. K., & Broström, G. (2018). On the variability in the onset of the Norwegian coastal current. *Journal of Physical Oceanography*, 48(3), 723–738. <https://doi.org/10.1175/jpo-d-17-0117.1>
- Copernicus Climate Change Service (C3S). (2017). ERA5: Fifth generation of ECMWF atmospheric reanalyses of the global climate Copernicus climate change Service climate data store (CDS). <https://doi.org/10.24381/cds.f17050d7>
- Crocker, R., Maksymczuk, J., Mittermaier, M., Tonani, M., & Péquignot, A.-C. (2020). An approach to the verification of high-resolution ocean models using spatial methods. *Ocean Science*, 16, 831–845. <https://doi.org/10.5194/os-16-831-2020>
- Davies, A. M., & Heaps, N. S. (1980). Influence of the Norwegian trench on the wind-driven circulation of the north sea. *Tellus*, 32(2), 164–175. <https://doi.org/10.3402/tellusa.v32i2.10491>
- Degraer, S., Van Lancker, V., Van Dijk, T. A. G. P., Birchenough, S. N. R., De Witte, B., Elliott, M., et al. (2019). Interdisciplinary science to support North Sea marine management: Lessons learned and future demands. *Hydrobiologia*, 845(1), 1–11. <https://doi.org/10.1007/s10750-019-04109-9>
- Desbiolles, F., Blanke, B., Bentamy, A., & Grima, N. (2014). Origin of fine-scale wind stress curl structures in the Benguela and Canary upwelling systems. *Journal of Geophysical Research: Oceans*, 119(11), 7931–7948. <https://doi.org/10.1002/2014jc010015>
- Ebisuzaki, W. (1997). A method to estimate the statistical significance of a correlation when the data are serially correlated. *Journal of Climate*, 10, 2147–2153. [https://doi.org/10.1175/1520-0442\(1997\)010<2147:amtets>2.0.co;2](https://doi.org/10.1175/1520-0442(1997)010<2147:amtets>2.0.co;2)
- Fossum, I. (2006). Analysis of instability and mesoscale motion off southern Norway. *Journal of Geophysical Research*, 111(C8), C08006. <https://doi.org/10.1029/2005jc003228>
- Frankignoulle, M., & Borges, A. V. (2001). European continental shelf as a significant sink for atmospheric carbon dioxide. *Global Biogeochemical Cycles*, 15(3), 569–576. <https://doi.org/10.1029/2000gb001307>
- Furnes, G. K. (1980). Wind effects in the north sea. *Journal of Physical Oceanography*, 10, 978–984. [https://doi.org/10.1175/1520-0485\(1980\)010<0978:weints>2.0.co;2](https://doi.org/10.1175/1520-0485(1980)010<0978:weints>2.0.co;2)
- Graham, J. A., Rosser, J. P., O’Dea, E., & Hewitt, H. T. (2018). Resolving shelf break exchange around the European northwest shelf. *Geophysical Research Letters*, 45(22), 12386–12395. <https://doi.org/10.1029/2018gl079399>
- Haid, V., Stanev, E. V., Pein, J., Staneva, J., & Chen, W. (2020). Secondary circulation in shallow ocean straits: Observations and numerical modeling of the Danish Straits. *Ocean Modelling*, 148. <https://doi.org/10.1016/j.ocemod.2020.101585>
- Halpern, B. S., Walbridge, S., Selkoe, K. A., Kappel, C. V., Micheli, F., D’Agrosa, C., et al. (2008). A global map of human impact on marine ecosystems. *Science*, 319(5865), 948–952. <https://doi.org/10.1126/science.1149345>
- Holt, J., Hughes, S., Hopkins, J., Wakelin, S. L., Holliday, N. P., Dye, S., et al. (2012). Multi-decadal variability and trends in the temperature of the northwest European continental shelf: A model-data synthesis. *Progress in Oceanography*, 106, 96–117. <https://doi.org/10.1016/j.pocean.2012.08.001>
- Holt, J., Polton, J., Huthnance, J., Wakelin, S., ODea, E., Harle, J., et al. (2018). Climate-driven change in the north Atlantic and Arctic ocean can greatly reduce the circulation of the north sea. *Geophysical Research Letters*, 45, 11827–11836. <https://doi.org/10.1029/2018GL078878>
- Holt, J., Wakelin, S., & Huthnance, J. (2009). Down-welling circulation of the northwest European continental shelf: A driving mechanism for the continental shelf pump. *Geophysical Research Letters*, 36, L14602. <https://doi.org/10.1029/2009GL038997>
- Hurrell, J., & National Center for Atmospheric Research Staff. (Ed.) Last modified 24 Apr 2020. The climate data Guide: Hurrell North Atlantic oscillation (NAO) index (station-based). Retrieved from <https://climatedataguide.ucar.edu/climate-data/hurrell-north-atlantic-oscillation-nao-index-station-based>
- Huthnance, J. (1991). Physical oceanography of the north sea. *Ocean and Shoreline Management*, 16(3–4), 199–231. [https://doi.org/10.1016/0951-8312\(91\)90005-m](https://doi.org/10.1016/0951-8312(91)90005-m)
- Iversen, E., & Burningham, H. (2015). Relationship between NAO and wind climate over Norway. *Climate Research*, 63(2), 115–134. <https://doi.org/10.3354/cr01277>
- Jacob, B., & Stanev, E. V. (2017). Interactions between wind and tidally induced currents in coastal and shelf basins. *Ocean Dynamics*, 67, 1263–1281. <https://doi.org/10.1007/s10236-017-1093-9>

- Jin, X., Dong, C., Kurian, J., McWilliams, J. C., Chelton, D. B., & Li, Z. (2009). SST–Wind interaction in coastal upwelling: Oceanic simulation with empirical coupling. *Journal of Physical Oceanography*, 39(11), 2957–2970. <https://doi.org/10.1175/2009jpo4205.1>
- Johannessen, J., Sandven, S., Lygre, K., Svendsen, E., & Johannessen, O. (1989). Three-dimensional structure of mesoscale eddies in the Norwegian Coastal Current. *Journal of Physical Oceanography*, (Vol. 19, pp. 32–19). [https://doi.org/10.1175/1520-0485\(1989\)019<0003:tdsome>2.0.co;2](https://doi.org/10.1175/1520-0485(1989)019<0003:tdsome>2.0.co;2)
- Johnson, C., Inall, M., Gary, S., & Cunningham, S. (2020). Significance of climate indices to benthic conditions across the Northern North Atlantic and adjacent shelf seas. *Frontiers in Marine Science*, 7, 2. <https://doi.org/10.3389/fmars.2020.00002>
- Karagali, I., Badger, M., Hahmann, A. N., Peña, A., Hasager, B. C., & Sempreviva, A. M. (2013). Spatial and temporal variability of winds in the Northern European Seas. *Renewable Energy*, 57, 200–210. <https://doi.org/10.1016/j.renene.2013.01.017>
- Kühn, W., Pätsch, J., Thomas, H., Borges, A. V., Schiettecatte, L.-S., Bozec, Y., & Prowe, A. E. F. (2010). Nitrogen and carbon cycling in the North Sea and exchange with the North Atlantic—a model study, Part II: Carbon budget and fluxes. *Continental Shelf Research*, 30(16), 1701–1716
- Legard, K. R., & Thomas, A. C. (2007). Spatial patterns of intraseasonal variability of chlorophyll and sea surface temperature in the California Current. *Journal of Geophysical Research*, 112(C9), C09006. <https://doi.org/10.1029/2007jc004097>
- Lewis, H., Castillo Sanchez, J. M., Siddorn, J., King, R., Tonani, M., Sautler, A., et al. (2019). Can wave coupling improve operational regional ocean forecasts for the North-West European Shelf. *Ocean Science*, 15, 669–690. <https://doi.org/10.5194/os-15-669-2019>
- Madec, G., and the NEMO team. (2016). *NEMO ocean engine, Note du Pôle de modélisation, No. 27*. Institut Pierre-Simon Laplace (IPSL), France. ISSN 1288-1619.
- Marsh, R., Haigh, I. D., Cunningham, S. A., Inall, M. E., Porter, M., & Moat, B. I. (2017). Large-scale forcing of the European slope current and associated inflows to the north sea. *Ocean Science*, 13(2), 315–335. <https://doi.org/10.5194/os-13-315-2017>
- Mathis, M., Elizalde, A., & Mikolajewicz, U. (2019). The future regime of Atlantic nutrient supply to the Northwest European Shelf. *Journal of Marine Systems*, 189, 98–115. <https://doi.org/10.1016/j.jmarsys.2018.10.002>
- Moullec, F., Asselot, R., Auch, D., Blöcker, A. M., Börner, G., Färber, L., et al. (2021). Identifying and addressing the anthropogenic drivers of global change in the north sea: A systematic map protocol. *Environmental Evidence*, 10(1), 1–11. <https://doi.org/10.1186/s13750-021-00234-y>
- NOOS Team. (2013). Exchange of computed water, salt, and heat transports across selected transects. Retrieved from [http://noos.eurogoos.eu/download/exch\\_transports\\_NOOS-BOOS\\_2013-08-30.pdf](http://noos.eurogoos.eu/download/exch_transports_NOOS-BOOS_2013-08-30.pdf)
- North-West Shelf Monitoring Forecasting Center. (2020). Atlantic- European North-West Shelf- Ocean Physics Reanalysis Product, E.U. Copernicus Marine Service Information [NWSHELF\_MULTIYEAR\_PHY\_004\_013]. Retrieved from [https://resources.marine.copernicus.eu/?option=com\\_csw&view=details&product\\_id=NORTHWESTSHELF\\_ANALYSIS\\_FORECAST\\_PHY\\_004\\_013](https://resources.marine.copernicus.eu/?option=com_csw&view=details&product_id=NORTHWESTSHELF_ANALYSIS_FORECAST_PHY_004_013)
- North-West Shelf Monitoring Forecasting Center. (2021). Atlantic- European North-West Shelf- Ocean Physics Reanalysis Product, E.U. Copernicus Marine Service Information [NWSHELF\_MULTIYEAR\_PHY\_004\_009]. Retrieved from [https://resources.marine.copernicus.eu/?option=com\\_csw&view=details&product\\_id=NWSHELF\\_MULTIYEAR\\_PHY\\_004\\_009](https://resources.marine.copernicus.eu/?option=com_csw&view=details&product_id=NWSHELF_MULTIYEAR_PHY_004_009)
- O’Dea, E., Furner, R., Wakelin, S., Siddorn, J., While, J., Sykes, P., et al. (2017). The CO5 configuration of the 7 km Atlantic Margin Model: Large-scale biases and sensitivity to forcing, physics options and vertical resolution. *Geoscientific Model Development*, 10(8), 2947–2969
- O’Neill, L. W., Chelton, D. B., & Esbensen, S. K. (2010). The effects of SST-induced surface wind speed and direction gradients on midlatitude surface vorticity and divergence. *Journal of Climate*, 23(2), 255–281
- Otto, L., Zimmerman, J. T. E., Furnes, G. K., Mork, M., Saetre, R., & Becker, G. (1990). Review of the physical oceanography of the North sea. *Netherlands Journal of Sea Research*, 26, 161–238. Issues 2. [https://doi.org/10.1016/0077-7579\(90\)90091-T](https://doi.org/10.1016/0077-7579(90)90091-T)
- Pätsch, J., Gouretski, V., Hinrichs, I., & Koul, V. (2020). Distinct mechanisms underlying interannual to decadal variability of observed salinity and nutrient concentration in the northern North sea. *Journal of Geophysical Research: Oceans*, 125(5). <https://doi.org/10.1029/2019JC015825>
- Pätsch, J., & Kühn, W. (2008). Nitrogen and carbon cycling in the North Sea and exchange with the North Atlantic—a model study. Part I. Nitrogen budget and fluxes. *Continental Shelf Research*, 28(6), 767–787. <https://doi.org/10.1016/j.csr.2007.12.013>
- Pryor, S. C., Schoof, J. T., & Barthelmie, R. J. (2006). Winds of change?: Projections of near-surface winds under climate change scenarios. *Geophysical Research Letters*, 33(11). <https://doi.org/10.1029/2006gl026000>
- Røed, L. P., & Fossum, I. (2004). Mean and eddy motion in the Skagerrak/northern North Sea: Insight from a numerical model. *Ocean Dynamics*, 54(2), 197–220. <https://doi.org/10.1007/s10236-003-0076-1>
- Sheehan, P. M. F., Berx, B., Gallego, A., Hall, R. A., Heywood, K. J., & Hughes, S. L. (2017). Thermohaline forcing and interannual variability of northwestern inflows into the northern North Sea. *Continental Shelf Research*, 138, 120–131. <https://doi.org/10.1016/j.csr.2017.01.016>
- Stanev, E. V., Badewien, T. H., Freund, H., Grayek, S., Hahner, F., Meyerjürgens, J., et al. (2019). Extreme westward surface drift in the North Sea: Public reports of stranded drifters and Lagrangian tracking. *Continental Shelf Research*, 177, 24–32. <https://doi.org/10.1016/j.csr.2019.03.003>
- Stanev, E. V., Pein, J., Grashorn, S., Zhang, Y., & Schrum, C. (2018). Dynamics of the Baltic Sea straits via numerical simulation of exchange flows. *Ocean Modelling*, 131, 40–58. <https://doi.org/10.1016/j.ocemod.2018.08.009>
- Thomas, H., Bozec, Y., Borges, A. V., Elkalay, K., Frankignoulle, M., Schiettecatte, L.-S., et al. (2005). The carbon budget of the North Sea. *Biogeosciences*, 2, 87–96. <https://doi.org/10.5194/bg-2-87-2005>
- Tonani, M., Sykes, P., King, R. R., McConnell, N., Péquignot, A.-C., O’Dea, E., et al. (2019). The impact of a new high-resolution ocean model on the Met Office North-West European Shelf forecasting system. *Ocean Science*, 15(4), 1133–1158. <https://doi.org/10.5194/os-15-1133-2019>
- Wakelin, S. L., Artioli, Y., Holt, J. T., Butenschön, M., & Blackford, J. (2020). Controls on near-bed oxygen concentration on the Northwest European Continental Shelf under a potential future climate scenario. *Progress in Oceanography*, 187, 102400. <https://doi.org/10.1016/j.pocean.2020.102400>
- Wang, Y., & Castelao, R. M. (2016). Variability in the coupling between sea surface temperature and wind stress in the global coastal ocean. *Continental Shelf Research*, 125, 88–96. <https://doi.org/10.1016/j.csr.2016.07.011>
- Winther, N. G., & Johannessen, J. A. (2006). North Sea circulation: Atlantic inflow and its destination. *Journal of Geophysical Research*, 111(C12), C12018. <https://doi.org/10.1029/2005jc003310>
- Yu, Y., Wang, Y., Cao, L., Tang, R., & Chai, F. (2020). The ocean-atmosphere interaction over a summer upwelling system in the South China Sea. *Journal of Marine Systems*, 208, 103360. <https://doi.org/10.1016/j.jmarsys.2020.103360>